

Primordial Black Hole Merger Rate in Self-Interacting Dark Matter Halo Models

Saeed Fakhry,^{1,*} Mahdi Naseri,^{2,†} Javad T. Firouzjaee,^{2,3,‡} and Mehrdad Farhoudi^{1,§}

¹*Department of Physics, Shahid Beheshti University, Evin, Tehran 19839, Iran*

²*Department of Physics, K.N. Toosi University of Technology, P.O. Box 15875-4416, Tehran, Iran*

³*School of Physics, Institute for Research in Fundamental Sciences (IPM), P.O. Box 19395-5531, Tehran, Iran*

(Dated: June 14, 2021)

We study the merger rate of primordial black holes (PBHs) in the self-interacting dark matter (SIDM) halo models. To explore a numerical description for the density profile of the SIDM halo models, we use the result of a previously performed simulation for the SIDM halo models with $\sigma/m = 10 \text{ cm}^2\text{g}^{-1}$. We also propose a concentration-mass-time relation that can explain the evolution of the halo density profile related to the SIDM models. Furthermore, we investigate the encounter condition of PBHs that may have been distributed in the medium of dark matter halos randomly. Under these assumptions, we calculate the merger rate of PBHs within each halo considering the SIDM halo models and compare the results with the one obtained for the cold dark matter (CDM) halo models. We indicate that the merger rate of PBHs for the SIDM halo models during the first epoch (i.e., $\Delta t \leq 1 \text{ Gyr}$ after the halo virialization) should be lower than the corresponding result for the CDM halo models, while by the time entering the second epoch (i.e., $\Delta t > 1 \text{ Gyr}$ after the halo virialization) sufficient PBH mergers in the SIDM halo models can be generated and even exceed the one resulted from the CDM halo models. By considering the spherical-collapse halo mass function, we obtain similar results for the cumulative merger rate of PBHs. Moreover, we calculate the redshift evolution of the PBH total merger rate. To determine a constraint on the PBH abundance, we study the merger rate of PBHs in terms of their fraction and masses and compare those with the black hole merger rate estimated by the Advanced LIGO (aLIGO) detectors during the third observing run. The results demonstrate that within the context of the SIDM halo models during the second epoch, the merger rate of $10 M_{\odot} - 10 M_{\odot}$ events falls within the aLIGO window. We also estimate a relation between the fraction of PBHs and their masses, which is well consistent with our findings.

PACS numbers: 97.60.Lf; 04.25.dg; 95.35.+d; 98.62.Gq.

Keywords: Primordial Black Hole; Self-Interacting Dark Matter; Merger Rate Per Halo.

I. INTRODUCTION

Over the past few years, the Laser Interferometer Gravitational-Wave Observatory (LIGO)/Virgo collaboration has detected gravitational waves emitted by about 50 inspiraling and merging black hole binaries [1–6] that have opened a new epoch in probing the nature and behavior of compact objects in the Universe. Interestingly, most of the black hole mergers recorded by the LIGO detectors are related to the black holes with masses around $30 M_{\odot}$. This fact certainly provides suggestive information of the mass distribution of black holes in the Universe.

Still, we do not know much about the origin of these black holes. There is a possibility that those are ordinary astrophysical black holes from stellar collapses (possibly from different channels) [7, 8]. The other interesting conjecture is that the LIGO detectors have detected primordial black holes (PBHs). These gravitational wave observatories are continuing to probe the population of black

holes, seeking to specify whether the mergers provide any direct evidence for the existence of PBHs or not.

The PBHs could have been formed in an early period of the evolution of the Universe as a consequence of the gravitational collapse of cosmological perturbations [9, 10]. By such a hypothesis, the PBHs can be generated due to high nonlinear rare peaks in the primordial distribution of density perturbations produced during the inflationary era. These perturbations can finally collapse when reentering the horizon, and produce black holes during the radiation domination era and/or some transitional matter phase. To form PBHs, these cosmological perturbations need to have some critical states. Passing from the threshold value of the density is the critical state of formation. Many numerical investigations have been performed to study the threshold value for the density perturbations, see, e.g., Refs. [10–17].

Before the detection of gravitational waves, many works have been done on the subject of PBHs as a candidate for dark matter, see, e.g., Ref. [18] and references therein. This issue comes from the fact that the massive PBHs interact only via gravitation, and since a large number of black holes have fluid behavior on sufficiently large scales, the PBHs are a natural campaigner for dark matter. However nowadays, the very strong observational limits on the abundance of PBHs mean themselves a powerful and unique method of investigating the early

*Electronic address: s.fakhry@sbu.ac.ir

†Electronic address: mahdi.naseri@email.kntu.ac.ir

‡Electronic address: firouzjaee@kntu.ac.ir

§Electronic address: m-farhoudi@sbu.ac.ir

Universe at small scales, which cannot be tested by any other method [19–21]. Nevertheless, the existence possibility of PBHs is yet neither proven nor refuted.

Assuming involving PBHs in merging pairs, serious bounds on the abundance of PBHs in the mass range around $10 - 30 M_{\odot}$ can be obtained from the LIGO observations. Shortly after the first observation of a binary black hole merger, several groups of researchers claimed that the merger rate by the LIGO/Virgo discovery is potentially consistent with a mass fraction of PBHs accounting for the total of dark matter [22–24]. The main assumption of their studies was that any two involved black holes had a primordial origin and the LIGO detectors had detected dark matter. Assuming that PBHs be a fraction of dark matter and their merging happens in the dark matter halo, the halo mass function can affect the merger rate of PBHs [25]. Also, any change in the concentration parameter can have an effect on the relative velocity distribution of PBHs within each halo, which determines the PBH merger rate within each halo. Accordingly, one can expect that different dark matter halo models can have a different prediction of the PBH merger rates.

One of the most renowned dark matter halo models is the self-interacting dark matter (SIDM) halo model which can resolve many astrophysical problems [26], and has rapidly turned into an interesting alternative for the cold dark matter (CDM) halo model. One of the famous examples of these problems is the “core-cusp problem”, which stems from a discrepancy between the observations and the CDM simulations for the halo density profiles. That is, the CDM simulations indicate a steep slope (cusp) of density profile at the central region of halos, however, the observed rotational curves of stars in galaxies reveal very low slope (core) in density profile.

The “missing satellite problem” is another challenge for the CDM paradigm. The CDM simulations predict the existence of a myriad of subhalos around the Milky Way (approximately 500 dwarf spheroidal galaxies [27]), yet the number of the observed dwarf spheroidal galaxies is only approximately 50 till now [28]. These problems can be solved considering a collisional type of dark matter with a non-negligible cross section per unit mass of particles instead of collisionless CDM. Since dark matter particles have a non-negligible cross section in the SIDM halos, those can interact with themselves. As a result, one can see the dependency of the halo density profile on the dark matter cross section [29]. Indeed, it has been established [26] that such an assumption may result in a heat transfer, which reduces the density of the central region of halos and consequently, eliminates the core-cusp problem. The capability of interaction with the other dark matter particles inside halos also leads to the formation of fewer satellites, and removes the missing satellite problem.

Considering hard-sphere scattering as the type of collision among the dark matter particles, the primary role in determining the SIDM properties is played by the con-

stant parameter of σ/m , that is the value of cross section per unit mass of dark matter particles. Alternatively, σ/m can depend on the velocity and interacts via a Yukawa potential [30]. The collisional dark matter that is studied in this work has a fixed σ/m and does not change with the velocity.

In this work, we propose to use the SIDM halo models to calculate the merger rate of PBHs. In this respect, the outline of the work is as follow. In Sec. II, we propose a halo model for the SIDM scenario, which includes a convenient density profile, concentration-mass-time relation and the spherical-collapse halo mass function. Then, in Sec. III, we calculate the merger rate of PBHs in the SIDM halo models, and compare it with the corresponding results of the CDM halo models. Also, we explore the redshift evolution of the PBH merger rate for the SIDM halo models, and compare it with the findings from the CDM halo models. Furthermore, we present constraints on the fraction of PBHs arising from the SIDM models. Finally, we discuss the results and summarize the findings in Sec. IV.

II. HALO MODELS

A. Halo Density Profile

For the CDM halo models, many simulations have been performed and resulted in some functions for their density profile. One of the most famous and successful density profiles was proposed by Navarro-Frenk-White (NFW) [31], which has the form of

$$\frac{\rho}{\rho_s} = \frac{1}{x(1+x)^2}, \quad (1)$$

where $x \equiv r/r_s$, and r_s is considered as the scale radius of the halo. In addition, ρ_s is given by $\rho_s = \rho_{\text{crit}} \delta_c$ for each halo, where ρ_{crit} is the critical density of the Universe at given redshift z and δ_c is the linear threshold of overdensities that depends on the concentration parameter C with the relation

$$\delta_c = \frac{200}{3} \frac{C^3}{\ln(1+C) - C/(1+C)}. \quad (2)$$

The concentration parameter is basically defined as the ratio of the virial radius of the halo, r_{vir} , to its scale radius, r_s . On the other hand, r_{200} is defined as the radius of the volume inside which the mean density is roughly equal to 200 times the critical density of the Universe. This radius is usually considered close to the virial radius of the halo, as the overdensity of the halo at the time of virialization is close to approximately 200 [32]. Therefore, the concentration parameter is

$$C \equiv \frac{r_{\text{vir}}}{r_s} \simeq \frac{r_{200}}{r_s}. \quad (3)$$

It can be deduced from Eq. (1) that the NFW density profile predicts $\rho \propto r^{-1}$ when $x \rightarrow 0$, whereas the density

changes with radius as $\rho \propto r^{-3}$ when $x \rightarrow \infty$. The SIDM simulations are significantly different than the CDM simulations of density profile and consequently, do not agree with the NFW behavior. One of the SIDM simulations has been performed by Fischer *et al.* and its outcome was provided in Fig. (5) of Ref. [33]. This simulation includes the SIDM particles with the cross section per unit mass of $\sigma/m = 10 \text{ cm}^2\text{g}^{-1}$. According to its results, the density profile gradually deviates from the NFW one at the inner region of the halo, and becomes cored by 1 Gyr after the halo virialization time. After this time, the central density grows with time, due to the fact that self-interactions among dark matter particles lead to energy transfer from the inner region to the outer parts of the halo. The core contracts due to this energy loss, and slowly becomes denser at the center, which is the so-called gravothermal core-collapse in the literature [33].

Our first task in this work is to find a quantitative description for density profile of SIDM halo models for calculating the merger rate of PBHs while assuming that the dark matter particles interact with themselves. In fact, the main effect of the SIDM halo models in our study stems from the evolution of the halo density profile. For this purpose, we try to specify a function that fits the result of the mentioned simulation. This issue can be performed by exerting some modifications to the NFW density profile.

The behavior of the density profile before and after core formation is substantially different. Therefore, we have divided the problem into two epochs, before and after 1 Gyr elapsed from the halo virialization time. Under these considerations, for the first epoch, i.e. $\Delta t \leq 1$ Gyr, we have taken the following form of the density profile

$$f(x) = \frac{\rho}{\rho_s} = \frac{1 + G_{11}(1 - \alpha_1)e^{-x/l_1}}{x^{\alpha_1}(1 + G_{12}x)^{3-\alpha_1+\beta_1}}, \quad (4)$$

where G_{11} , G_{12} , α_1 , β_1 and l_1 are free parameters to be determined. We have found some numerical suggestions in a way to have three criteria as: (i) The density profile being reduced to the NFW one at $\Delta t = 0$; (ii) It forms core at $\Delta t = 1$ Gyr; (iii) It continuously changes in this interval. Clearly, all those free parameters are only functions of Δt , because the evolution of the density profile in the SIDM halos depends only on the time elapsed from the halo virialization. Under these conditions, one can set the free parameters of relation (4) to be

$$\begin{aligned} \alpha_1 &= 1 - \Delta t, & \beta_1 &= \Delta t, & l_1 &= 4, \\ G_{11} &= 24 \exp \left[- \left(\frac{\Delta t - 1.938}{1.148} \right)^2 \right], & & & & (5) \\ G_{12} &= 0.6\Delta t + 1. \end{aligned}$$

Then, we have iterated this method for the second epoch, i.e., $\Delta t > 1$ Gyr. Accordingly, the second function must continuously change from the cored shape until forming

the third plot in Fig. (5) of Ref. [33] at $\Delta t = 4$ Gyr. Furthermore, both functions must reduce to each other at $\Delta t = 1$ Gyr for continuity condition. Hence, under these conditions, the density profile for the second epoch, i.e., $\Delta t > 1$ Gyr, sets to be

$$f(x) = \frac{\rho}{\rho_s} = \frac{1 + G_{21}(1 - \alpha_2)e^{-x/l_2}}{x^{\alpha_2}(1 + G_{22}x)^{3-\alpha_2+\beta_2}}, \quad (6)$$

where G_{21} , G_{22} , α_2 , β_2 and l_2 are also free parameters to be determined. Similarly, to specify the best fit of the density profile simulated in Ref. [33], we have also suggested the expressions for those free parameters to be

$$\begin{aligned} \alpha_2 &= 0, & \beta_2 &= 1, & l_2 &= 4, \\ G_{21} &= 12.3\Delta t^{1.75}, & & & & (7) \end{aligned}$$

$$G_{22} = 11.38 \exp \left[- \left(\frac{\Delta t - 9.544}{6.11} \right)^2 \right].$$

The resulted density profiles, i.e., Eqs. (4) and (6), have been illustrated in Fig. 1 for different Δt values. Comparing this figure with the obtained result in Ref. [33] shows that our suggested density profile and its parameters are in a good agreement with the mentioned simulation.

To find more exact expressions for the parameters of the proposed density profiles, the repetition of the simulation for a number of Δt values is required. Moreover, the simulation has been conducted for the SIDM particles with cross section per unit mass of $\sigma/m = 10 \text{ cm}^2\text{g}^{-1}$. It means that the proposed density profiles are only acceptable for this value. However, many other simulations predict that the lower values of σ/m merely affect the speed of core formation and core-collapse [34]. In other words, the shapes of the profiles do not change as every stage occurs at a later time compared with $\sigma/m = 10 \text{ cm}^2\text{g}^{-1}$. However, there is an exception, i.e., the effects of the SIDM interactions are negligible for a lower limit of cross section per unit mass of the dark matter particle. Thus, for very small values of σ/m , deviation from the NFW profile is not considerable. Clearly, in the purposed studying of the impact of the SIDM on any astrophysical phenomenon, the dark matter particles are considered to have larger cross section than the lower limit (which has different values in various studies), otherwise, there would be no observable difference between the CDM and the SIDM halo models.

B. Halo Concentration-Mass-Time Relation

The primary conclusion of studying the density profiles of the SIDM halo models reveals that, while the density profile remains unchanged with time in the CDM halo models, it dramatically changes with time for the SIDM halo models. Such a difference means that the concentration parameter is not time-independent anymore and changes with time for the SIDM halos.

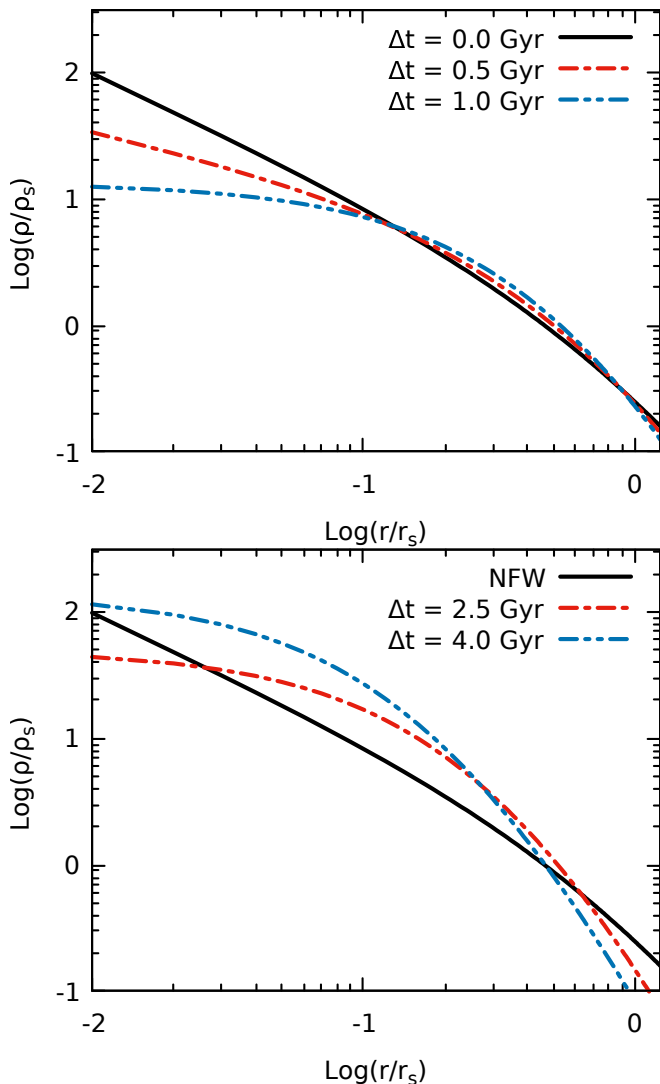


FIG. 1: (color online) The density profiles of Eqs. (4) and (6) for several times after the halo virialization for the SIDM halo models. The top plot reveals how the density profile becomes cored before $\Delta t = 1$ Gyr, and the bottom plot shows how it changes after this time. At $\Delta t = 0$, the proposed profile overlaps the NFW density profile. The NFW density profile has also been displayed in the bottom panel for comparison.

In addition, the N -body simulations indicate that the concentration parameter is a decreasing function of the halo mass [35–38]. For the CDM halo models, a relation has been obtained between the concentration parameter and the halo mass as [39]

$$C_{\text{NFW}} = 8.3 \left(\frac{M_{200}}{10^{12} h^{-1} M_{\odot}} \right)^{-0.104}. \quad (8)$$

Here, M_{200} is the mass enclosed by the radius of r_{200} , which is usually close to the virial mass, M_{vir} , at the halo virialization time [32].

It should be noted that the scale radius of a halo, r_s , is defined as the radius at which the logarithmic slope

of density profile is -2 , i.e., $\rho(x_s) \propto x^{-2}$ [40]. In order to determine the scale radius in the proposed density profiles, the method provided in Ref. [41] can be used. Hence, we have demanded that the logarithmic slope of the density distribution to be -2 at the scale radius, that is

$$\left. \frac{d \ln \rho(x)}{d \ln(x)} \right|_{x=x_s} = \left. \frac{d \ln(x^{-2})}{dx} \right|_{x=1} = -2. \quad (9)$$

Accordingly, x_s can be obtained via numerical solution. As the density profile for both models (i.e., the CDM and the SIDM) is the same at the halo virialization time (i.e., at $\Delta t = 0$), r_{vir} is the same for both cases and C changes with r_s regarding Eq. (3). Therefore

$$\frac{C_{\text{NFW}}}{C} = \frac{r_s}{r_{s,\text{NFW}}} = x_s. \quad (10)$$

By specifying the scale radius via Eq. (9), relation (10) can be used together with relation (8) to calculate the halo concentration parameter for the given virialized mass M_{vir} and for time Δt after the halo virialization.

We have used the above method for several halo mass values and a range of times after the halo virialization, to calculate the concentration parameter, and then have tried to specify the best fit of $C(\Delta t, M_{\text{vir}})$ for the concentration-mass-time relation. The following function properly fits the result and can be considered as the concentration-mass-time relation for the SIDM halo models, namely

$$C_{\text{SIDM}} = \{k_1 \exp(k_2 \Delta t) + k_3\} \left(\frac{M_{\text{vir}}}{10^{14} h^{-1} M_{\odot}} \right)^{k_4}, \quad (11)$$

with $k_1 = 18.53$, $k_2 = 0.1951$, $k_3 = -12.84$ and $k_4 = -0.104$. The result has been depicted in Fig. 2 for three various halo masses. In agreement with many other studies [40, 42], the SIDM halo models lead to a more significant concentration parameter than the corresponding one obtained from the CDM halo models. Moreover, in order to calculate the redshift evolution of the concentration-mass relation, we have referred to the definition of the linear root-mean-square fluctuation of overdensities

$$\sigma(M, z) \equiv \frac{1}{2\pi^2} \int_0^{\infty} P(k, z) W^2(k, M) k^2 dk, \quad (12)$$

where $P(k, z)$ is the power spectrum of the fluctuations, and $W(k, M)$ is the Fourier spectrum of the top-hat filter that depends on the halo mass M and the wave number k . By this description, one can define a dimensionless parameter called the peak height, $\nu(M, z)$, as

$$\nu(M, z) \equiv \frac{\delta_c}{\sigma(M, z)}, \quad (13)$$

where $\delta_c = 1.686$ is the linear threshold of overdensities for the spherical-collapse halo models. Specifically, the peak height depends on the halo mass and redshift.

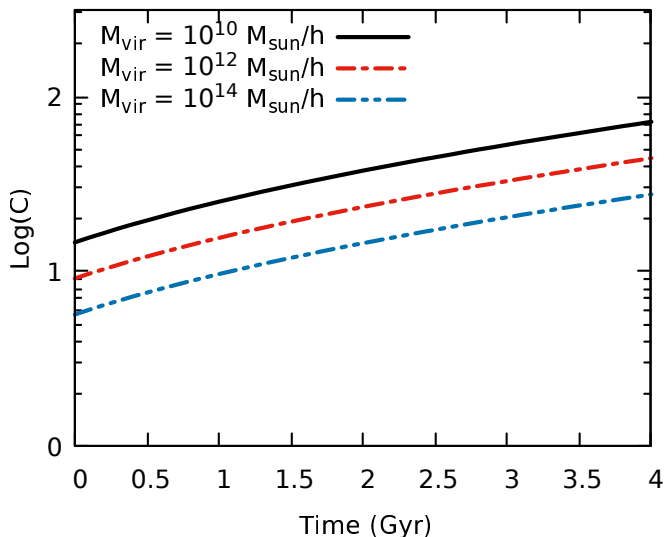


FIG. 2: (color online) The evolution of the concentration parameter with respect to the time after halo virialization. The solid (black) line, the dot-dashed (red) line and the dot-dot-dashed (blue) line show this relation for the virial masses of $M_{\text{vir}} = 10^{10}$, 10^{12} and $10^{14} h^{-1} M_{\odot}$, respectively.

On the other hand, for halo masses within the range of $10^{-7} \leq M_{\text{vir}}/(h^{-1} M_{\odot}) \leq 10^{15}$, the linear root-mean-square fluctuation of overdensities can be approximated as [38]

$$\sigma(M, z) \simeq D(z) \frac{22.26\chi^{0.292}}{1 + 1.53\chi^{0.275} + 3.36\chi^{0.198}}, \quad (14)$$

where $D(z)$ is the linear growth factor [43] and

$$\chi = \left(\frac{M_{\text{vir}}}{10^{10} h^{-1} M_{\odot}} \right)^{-1}. \quad (15)$$

Using relations (13), (14) and (15), one can calculate the peak height parameter in terms of the halo mass and the linear growth factor to be

$$\nu(M_{\text{vir}}, z) \simeq \frac{1}{D(z)} \sum_{i=1}^3 a_i \chi^{b_i}, \quad (16)$$

where $a_1 = 0.0757$, $a_2 = 0.254$, $a_3 = 0.115$, $b_1 = -0.292$, $b_2 = -0.094$ and $b_3 = -0.017$. Fig. 3 shows the peak height as a function of the halo mass and redshift. Eventually, using relation (16), one can achieve the $C(\nu)$ relation that enables us to provide the concentration parameter as a function of the halo mass and redshift. In particular, we will use this relation to determine the redshift evolution of the total merger rate of PBHs (see Sec. III B 2).

C. Halo Mass Function

Gravitational collapse is a suitable and crucial frame for modeling spherically symmetric overdensities that

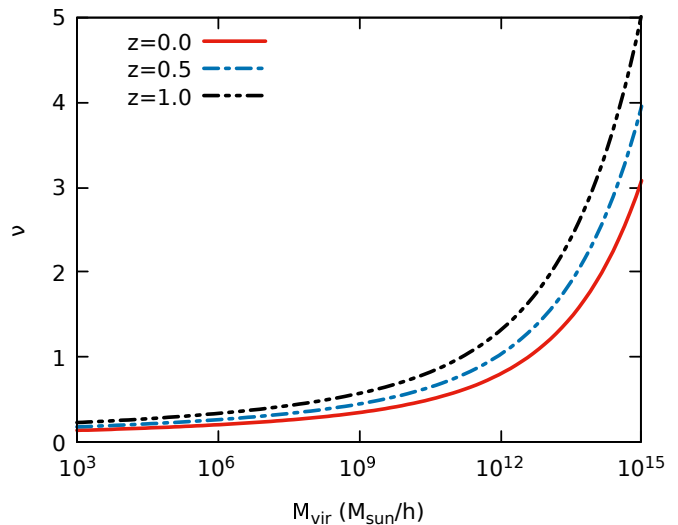


FIG. 3: (color online) The peak height as a function of the halo mass and redshift. The solid (red) line, the dot-dashed (blue) line and the dot-dot-dashed (black) line represent the $\nu(M)$ relation for $z = 0$, 0.5 and 1 , respectively.

lead to the formation of virialized dark matter halos. Therefore, having a suitable model based on the spherically symmetric gravitational collapse is necessary to describe the behavior of dark matter halos and to classify those based on their mass distribution. In this regard, a function called the halo mass function has been introduced in cosmology, which provides a well description of the mass distribution of dark matter halos [44–46].

The halo mass function is a powerful probe in cosmology and related theories. Hence, having a proper halo mass function with high prediction accuracy is an essential tool, and can be used as the initial assumption of simulations related to the formation of cosmic structures. In other words, the halo mass function describes structures whose densities exceed the threshold, decouple from the cosmological expansion and lead to gravitational collapse.

In cosmology, one can introduce a parameter called the density contrast, i.e., $\delta(x) \equiv [\rho(x) - \bar{\rho}]/\bar{\rho}$, where $\rho(x)$ is the local density at arbitrary point x and $\bar{\rho}$ is the average background energy density. The density contrast is a criterion for the local increase of density fluctuations. For this reason, it can indicate the conditions under which the structures will be formed.

As mentioned, a threshold value for the density contrast has been calculated in cosmology for the spherical-collapse halo models that is equal to $\delta_c = 1.686$. This value is independent of all local quantities such as mass and radius, and depends only on the redshift in a way that, in a narrow redshift range, it can be considered as a constant threshold [44].

On the other hand, to characterize various fits for dark matter halos, a convenient definition of the differential

halo mass function has been introduced in Ref. [47] as

$$\frac{dn}{dM} = f(\sigma) \frac{\rho_m}{M} \frac{d \ln(\sigma^{-1})}{dM}, \quad (17)$$

where $n(M)$ is the number density of dark matter halos, M is the halo mass, ρ_m is the cosmological matter density and $f(\sigma)$ is a function that is related to the geometrical conditions for the overdensities at the collapse time which can be derived from the mathematical approaches or numerical simulations.

Many studies have been performed to achieve an appropriate halo mass function with the aim of accurate predictions that can provide the best fit for the cosmic observations. One of the most successful models introduced for the halo mass function was performed by Press and Schechter [48]. Their formalism was based on an analytical approach assuming the homogeneous and isotropic gravitational collapse of overdensities. Under these assumptions, they have presented a suitable halo mass function as

$$f_{\text{P-S}}(\sigma) = \sqrt{\frac{2}{\pi}} \frac{\delta_{\text{sc}}}{\sigma} \exp\left(\frac{-\delta_{\text{sc}}^2}{2\sigma^2}\right), \quad (18)$$

which is known as the Press-Schechter (P-S) halo mass function. Such a formalism predicts how many dark matter halos could exist between the mass M and $M + dM$, assuming that the hierarchical structure formation occurs in objects with masses larger than M . In addition to the P-S formalism, other models have been proposed for the halo mass function based on numerical simulations and analytical approaches [45, 47, 49–51].

In this work, we consider the shape of halos to be spherical. This choice is well-justified by direct effects of the self interaction among dark matter particles, as simulations indicate that the SIDM halos are more spherical than the CDM ones [34]. A broad reserach on the SIDM halo shapes and comparing those with the observational data has been conducted in Ref. [52]. The result reveals that the SIDM halo models with higher values of σ/m are rounder than the CDM halo models, particularly in their inner region. The observed halo shape varies with respect to the various contributors, such as halo size and the definition of the halo shape. In fact, one of the observational constraints on the value of σ/m could be found through the shape of halos. For $\sigma/m > 1 \text{ cm}^2\text{g}^{-1}$, the spherical assumption is a natural consequence of the SIDM halo models. Under these considerations, we use the P-S mass function to calculate the merger rate of PBHs in the SIDM halo models.

Up to now, we have specified the framework for the SIDM halo models. Hence, we are able to study the merger rate of PBHs considering the SIDM halo models. For this purpose, we will discuss the encounter condition of PBHs in the medium of the dark matter halos, their binary formation conditions and their merger rates in the following section.

III. MERGER RATE OF PBHS

A. Merger Rate of PBHs Within Each Halo

In this section, we intend to calculate the merger rate of PBHs in the framework of the SIDM halo models. The PBHs are a special type of black holes that follow a different process of formation compared to the formation of black holes with astrophysical origin. Sufficiently dense regions in the early Universe may lead to the formation of PBHs shortly after the big bang due to the direct collapse of overdensities that exceeds their thresholds. In addition, the random distribution of PBHs in the dark matter halos allows those to form binaries not only during the radiation-dominated era but also in the late-time Universe.

As mentioned, it is believed that the detection of gravitational waves from a binary black hole merger via the LIGO detectors would be compatible with the merger rate of PBHs with a typical mass $30 M_{\odot}$, if a significant fraction of dark matter is formed by PBHs. In this work, we propose to interpret the conditions under which the stellar-mass PBHs (as a proposed candidate of dark matter) in the medium of dark matter halos could encounter each other, form binaries and eventually merge. In fact, our aim is to calculate the merger rate of PBHs in the SIDM halo models, and to compare it with the corresponding result of the CDM halo models.

Consider two PBHs with masses m_1 and m_2 and relative velocity at the large separation $v_{\text{rel}} = |v_1 - v_2|$ that suddenly encounter each other in a dark matter halo. Due to the maximum scattering amplitude, significant gravitational radiation would happen when those are located at the closest separation (i.e., at periastron) from each other. The time-average gravitational energy emitted from such an encounter can be calculated in the context of Keplerian mechanics [53] as

$$\left\langle \frac{dE_{\text{rad}}}{dt} \right\rangle = -\frac{32}{5} \frac{G^4 (m_1 m_2)^2 (m_1 + m_2)}{c^5 a^{3/2} r_p^{7/2} (1+e)^{7/2}} \left(1 + \frac{73}{24} e + \frac{37}{96} e^2 \right), \quad (19)$$

where G is the gravitational constant, c is the velocity of light, a and e are the semi-major axis and eccentricity of the orbit, and $r_p = a(1-e)$ is the periastron. Near the periastron, the trajectory can roughly be considered as an ellipse with the highest eccentricity (i.e., $e = 1$), for the strong gravitational limits dominate this binary in a way that the most gravitational radiation occurs at this point. Under these assumptions, one can calculate the radiated gravitational energy after one orbital period as

$$\Delta E_{\text{rad}} = \frac{85\pi}{12\sqrt{2}} \frac{(m_1 m_2)^2 \sqrt{(m_1 + m_2)}}{c^5 r_p^{7/2}}. \quad (20)$$

If the radiated gravitational energy is greater than the kinetic energy of those PBHs, then those will become gravitationally bound and form a binary. This condition leads to a maximum value for the periastron as

$$r_{p,\max} = \left[\frac{85\pi G^{7/2} m_1 m_2 (m_1 + m_2)^{3/2}}{6\sqrt{2} c^5 v_{\text{rel}}^2} \right]^{2/7}. \quad (21)$$

The implication of this maximum value is that those PBHs would be able to form a binary if the condition $r_p < r_{p,\max}$ can be satisfied. On the other hand, in the Newtonian approximation, the relation between the impact parameter b and the periastron can be obtained as [54]

$$b(r_p) = \frac{2G(m_1 + m_2)r_p}{v_{\text{rel}}^2} + r_p^2. \quad (22)$$

Moreover, for such an encounter, the merger cross section $\xi(m_1, m_2, v_{\text{rel}})$ is equal to the area of a circle with a radius of $b(r_{p,\max})$ [55, 56].

In this work, we are interested in studying the merger rate of PBHs that are consistent with the mergers obtained via the LIGO detectors, i.e., $30 M_\odot - 30 M_\odot$ events in the dark matter halos. For this purpose, we have considered binaries with equal-mass components, i.e., $m_1 = m_2 = M_{\text{PBH}}$, and have set $v_{\text{rel}} = v_{\text{PBH}}$. Under these assumptions and considering the strong limit of the gravitational focusing (i.e., $r_p \ll b$), the merger cross section ξ can be achieved as

$$\begin{aligned} \xi &\simeq 4\pi \left(\frac{85\pi}{3} \right)^{2/7} \left(\frac{M_{\text{PBH}}^2 G^2}{c^{10/7} v_{\text{PBH}}^{18/7}} \right) \\ &\simeq 1.37 \times 10^{-14} \left(\frac{M_{\text{PBH}}}{30 M_\odot} \right)^2 \left(\frac{v_{\text{PBH}}}{200 \text{ km/s}} \right)^{-18/7} \text{ in } (\text{pc})^2, \end{aligned} \quad (23)$$

where, in the last line, we have normalized the PBH mass to $30 M_\odot$ and the PBH relative velocity to average velocities of dark matter halos, i.e., 200 km/s. Accordingly, the merger rate of PBHs within each halo can be specified using the relation [22, 57]

$$\Gamma = 2\pi \int_0^{r_{\text{vir}}} r^2 \left(\frac{\rho(r)}{M_{\text{PBH}}} \right)^2 \langle \xi v_{\text{PBH}} \rangle dr, \quad (24)$$

where $\rho(r)$ is the halo density profile, and the angle bracket shows an average over the PBH relative velocity distribution in the galactic halo.

In addition, the mass bounded via the virial radius of the halo, the virialized mass, can be calculated as

$$M_{\text{vir}} = \int_0^{r_{\text{vir}}} 4\pi r^2 \rho(r) dr. \quad (25)$$

Another important factor in calculating the merger rate of PBHs is the halo velocity dispersion. It should be noted that the self-interacting scenario of dark matter only changes the velocity dispersion in the inner region of a halo and has no significant effect in outward radii, where the velocity dispersion reaches the maximum value

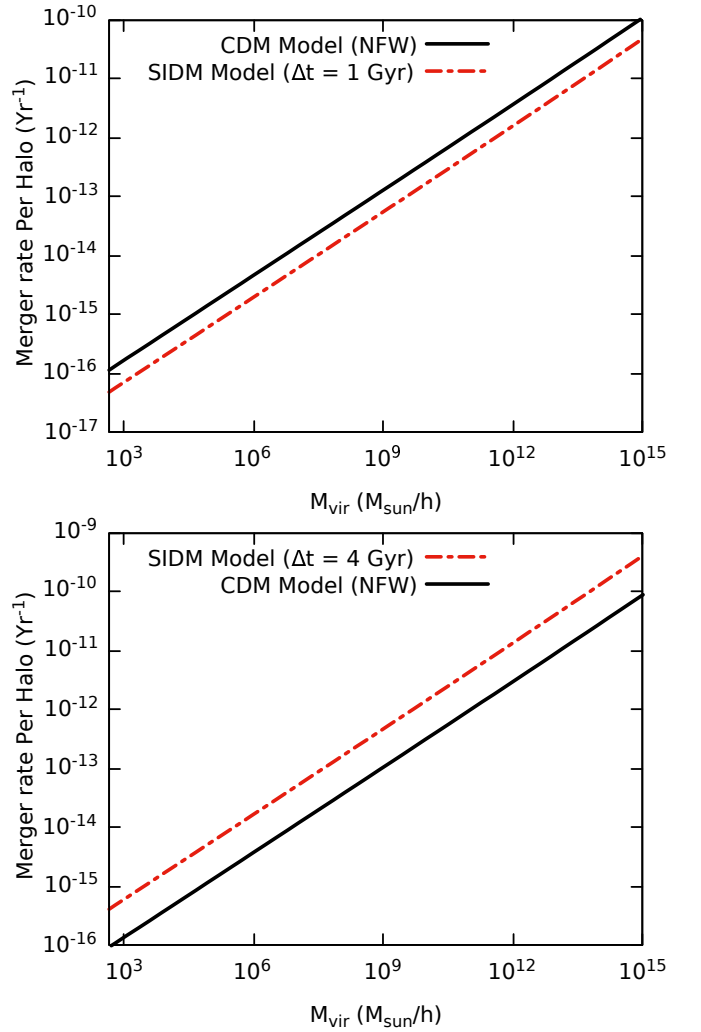


FIG. 4: (color online) The PBH merger rate within each halo for the SIDM and the CDM halo models. The dot-dashed (red) lines represent the merger rate of PBHs in the SIDM halo models for $\Delta t = 1$ Gyr (top) and $\Delta t = 4$ Gyr (bottom) after the halo virialization time, while the solid (black) lines show the CDM halo models with the NFW density profile.

[58]. Therefore, with a plausible approximation, one can use the relation obtained in Ref. [35] for the halo velocity dispersion, namely

$$v_{\text{disp}} = \frac{v_{\text{max}}}{\sqrt{2}} = \sqrt{\frac{GM(r < r_{\text{max}})}{r_{\text{max}}}}. \quad (26)$$

We have also demanded that the relative velocity distribution of PBHs in the galactic halo corresponds to the Maxwell-Boltzmann statistics with the following probability distribution function while considering a cutoff at the halo virial velocity, i.e.,

$$P(v_{\text{PBH}}, v_{\text{disp}}) = F_0 \left[\exp\left(-\frac{v_{\text{PBH}}^2}{v_{\text{disp}}^2}\right) - \exp\left(-\frac{v_{\text{vir}}^2}{v_{\text{disp}}^2}\right) \right], \quad (27)$$

where F_0 is specified by $4\pi \int_0^{v_{\text{vir}}} P(v)v^2 dv = 1$. It is clear from relations (4), (6) and (24) that the concentration parameter plays a crucial role in calculating the merger rate of PBHs within each halo. Hence, due to the fact that this parameter for the SIDM halo models deviates significantly from the one for the CDM halo models, it can be expected that the merger rate of PBHs within each halo for the SIDM halo models varies from the one obtained from the CDM halo models. Accordingly, in order to calculate the merger rate of PBHs for the SIDM models, we have used relation (11) for the concentration parameter, and have employed relation (8) to obtain the corresponding result for the CDM models. We have also set the mass of PBHs to be $30M_\odot$.

In Fig. 4, we have shown the merger rate of PBHs within each halo with respect to the halo mass for the SIDM models while considering two different times after the halo virialization, and have compared those with the corresponding result for the CDM models. It is clear from this figure that the merger rate per halo for the SIDM models with $\Delta t = 1$ Gyr after the halo virialization is lower than the merger rate for the CDM models, while the merger rate for $\Delta t = 4$ Gyr after the halo virialization in the SIDM models is higher than the one obtained from the CDM models.

The main reason of this difference is the time evolution of the halo density profile in the SIDM halo models. As can be seen in Fig. 1, the density profile inside the inner region of the SIDM halos becomes cored until $\Delta t = 1$ Gyr after the virialization time, and it is lower than the one in the CDM halos in the same time. On the contrary, density at the central region increases during $\Delta t > 1$ Gyr and at later epoch, e.g., $\Delta t = 4$ Gyr, the core is collapsed. At this stage, the inner region of the SIDM halos is much denser than the CDM halos. In addition, it is clear from relation (24) that the merger rate of PBHs is proportional to the density profile directly. Thus, as expected, the time evolution of density profile resulting from the SIDM halo models in the inner region of halos leads to a modification in the merger rate of PBHs residing in the dark matter halos.

In the following, we intend to study the effect of the SIDM halo models on the total merger rate of PBHs per unit time and per unit volume and compare it with the corresponding results of the CDM halo models.

B. Total Merger Rate of PBHs

1. Present-Time Universe

It should be noted that the accumulation of the binary black hole merger rates can be deduced from the data recorded by the gravitational wave detectors. The quantities we have explained till now are needed to achieve the cumulative merger rate of PBHs per unit time and per unit volume. Hence, to calculate the total merger rate of PBHs, the last step is to convolve the halo mass

function dn/dM_{vir} with the merger rate per halo $\Gamma(M_{\text{vir}})$. Under these considerations, the total merger rate can be obtained as

$$\mathcal{R} = \int_{M_{\text{min}}} \frac{dn}{dM_{\text{vir}}} \Gamma(M_{\text{vir}}) dM_{\text{vir}}. \quad (28)$$

We demand the initial conditions for the formation of both models, i.e., SIDM and CDM halo models, being the same based on a spherically symmetric gravitational collapse. Therefore, to achieve the total merger rate of PBHs, we have used the P-S halo mass function introduced in Sec. II C. Due to the presence of the exponential term in the P-S halo mass function, the upper limit of the halo mass has no significant effect on the final result, whereas the role of the lower limit of the halo mass is crucial. Because, it has been indicated that the subhalos must contain dark matter with lower velocity dispersion and higher density than the larger host halos [22, 27, 59]. In this regard, it is expected from relation (24) that the smallest halos have significant contribution to the merger rate of PBHs.

In addition, we assume that the merger rate of binaries consisting of non dissipative three-body encounters must be negligible. Because those often lead to wide binaries that do not have enough binding energy to merge during the age of the Universe [55]. As a result, their mergers could not be recorded by the LIGO detectors.

It is believed that the smallest halos evaporate faster than the larger halos because they have already become virialized. On the other hand, the time scale of halo evaporation depends on the number of independent objects that may reside in the halos (i.e., $N = M_{\text{vir}}/M_{\text{PBH}}$). It has been shown [22] that the evaporation time of halos with a mass of $400 M_\odot$, which include PBHs with a mass of $30 M_\odot$, is about 3 Gyr. On the other hand, the halo evaporation during the matter-dominated era is compensated by some processes, such as the accretion of surrounding materials into the halo or the merging of smaller halos. However, the compensating processes slow down during the dark energy dominated era (i.e., approximately 3 Gyr ago) due to the accelerating expansion of the Universe. As a result, it can be assumed that signals from the halos with an evaporation time of less than 3 Gyr are negligible. Hence, one can ignore the signal from the halos with masses less than $400 M_\odot$ (see, e.g., Refs. [22, 25] for more details). With this argument, we have set the lower limit of the halo mass to be $400 M_\odot$, while containing PBHs with a typical mass of $30 M_\odot$.

In Fig. 5, we have indicated the merger rate of PBHs per unit time and per unit volume for two different epochs after the halo virialization time in the SIDM halo models and have compared those with the one obtained from the CDM halo models. The figure shows that the merger rate of PBHs for both models decreases with increasing halo mass. This result is due to the presence of the exponential term in the halo mass function that well justifies the inverse evolution of the dark matter density and the direct evolution of the dark matter velocity dispersion

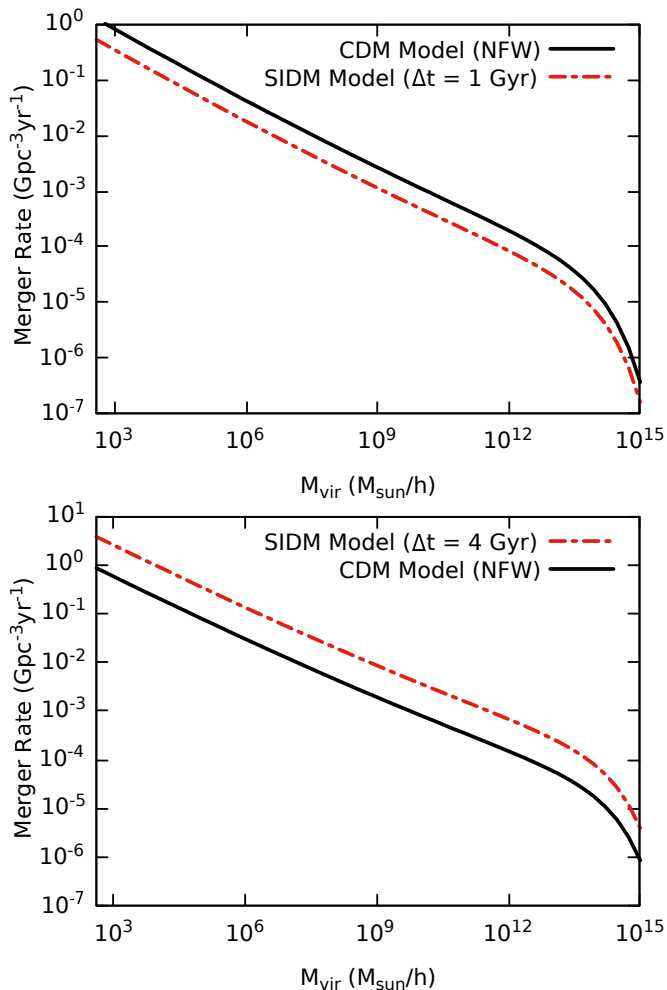


FIG. 5: (color online) The total merger event rate of PBHs per unit source time and per unit comoving volume for the SIDM and CDM halo models over the halo virial mass. The dot-dashed (red) lines represent the SIDM halo models for the $\Delta t = 1$ Gyr (top) and $\Delta t = 4$ Gyr (bottom) after halo virialization time. The solid (black) lines show the CDM halo models with the NFW density profile.

with the halo mass. Obviously, the merger rate of PBHs for the SIDM halo models after $\Delta t = 1$ Gyr from the halo virialization is lower than the corresponding result for the CDM halo models, whereas, after $\Delta t = 4$ Gyr from the halo virialization, the SIDM halo models can enhance the PBH merger rates in such a way that exceed the ones extracted from the CDM halo models.

2. Redshift Evolution of PBH Merger Rate

The history of the black hole merger rate during the evolution of the Universe is one of the suitable criteria to separate black hole formation scenarios [54]. Moreover, the development of instruments and increment of their accuracy can enable gravitational-wave detectors to probe events in higher redshifts. Nowadays, the Ad-

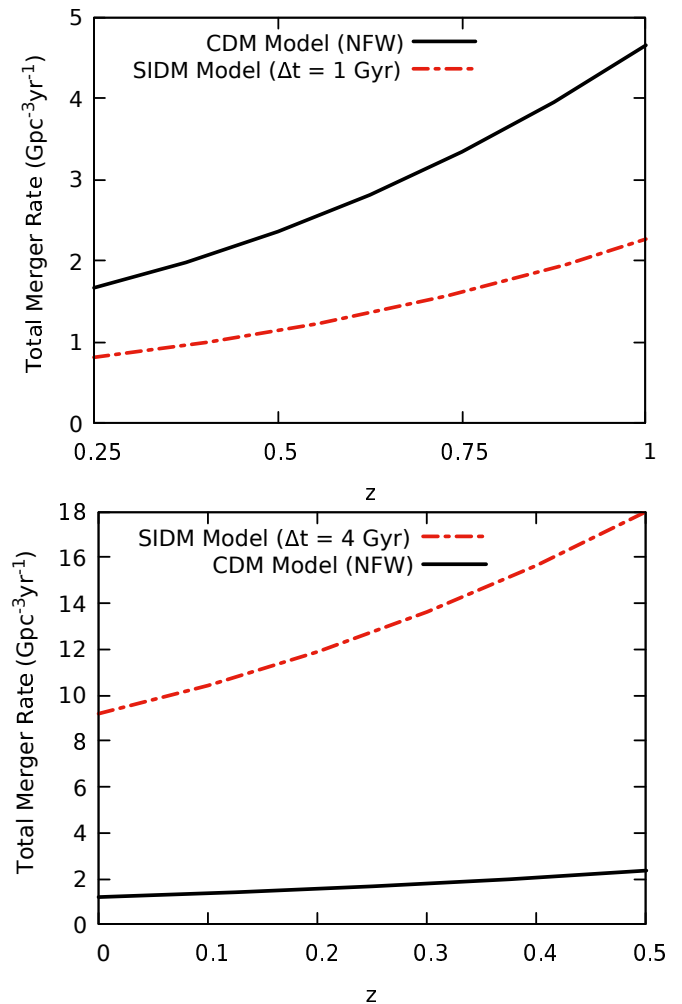


FIG. 6: (color online) The redshift evolution of the total merger rate of PBHs per unit source time and per unit comoving volume for the SIDM and the CDM halo models. The dot-dashed (red) lines represent the SIDM halo models for the $\Delta t = 1$ Gyr (top) and $\Delta t = 4$ Gyr (bottom) after halo virialization time, while the solid (black) lines show the CDM halo models with the NFW density profile.

vanced LIGO (aLIGO) detectors can detect binary mergers up to $z \sim 0.75$, which approximately corresponds to a comoving volume around 50 Gpc^3 [60, 61]. For this reason, we are going to discuss the evolution of the PBH merger rate as a function of redshift for the SIDM and the CDM halo models. In this regard, it is obvious that relation (28) depends on the redshift through the halo mass function and the concentration parameter [62].

Fig. 6 shows the redshift evolution of the total merger rate of PBHs for the SIDM and the CDM halo models. Specifically, the total merger rate of PBHs is directly proportional to the redshift for the both models. This result suggests that the PBHs have been more likely to form binaries at higher redshifts than the present-day Universe, which is compatible with other studies [25, 62, 63]. As can be seen from the top panel, the total merger

TABLE I: The total merger event rate of PBHs per unit source time and per unit comoving volume as a function of redshift for the SIDM and the CDM halo models. The mass of PBHs has been considered to be $30 M_{\odot}$.

Model	Redshift (z)	Total Merger Rate ($\text{Gpc}^{-3}\text{yr}^{-1}$)
CDM	0.0	1.20
	0.25	1.67
	0.50	2.36
	0.75	3.34
	1.0	4.65
SIDM ($\Delta t = 1$ Gyr)	0.25	0.81
	0.40	1.00
	0.55	1.23
	0.73	1.57
	0.89	1.95
	1.0	2.51
SIDM ($\Delta t = 4$ Gyr)	0.0	9.19
	0.1	10.42
	0.2	11.89
	0.3	13.62
	0.4	15.65
	0.5	17.99

rate of PBHs for the SIDM halo models after $\Delta t = 1$ Gyr from the halo virialization is lower than the one for the CDM halo models, while the bottom panel indicates that the SIDM halo models in $\Delta t = 4$ Gyr after the halo virialization strengthen the total merger rate of PBHs compared to the corresponding result obtained from the CDM halo models.

As a result, it can be inferred that the merger rate of PBHs will be amplified over time if the SIDM halo models are reliable. In other words, due to the time evolution of density profile, the merger rate of PBHs in the SIDM models evolves in a way that is quite different rather than the evolutionary behavior of the merger rate of PBHs derived from the CDM models. This result can be validated as a distinguishing feature between the SIDM and the CDM halo models. Information on the redshift evolution of the merger rate of PBHs per unit source time and per unit comoving volume has been provided in Table I for the SIDM and the CDM halo models.

3. Constraint on PBH Fraction

The study of constraints arising from the effects of PBHs on the observable Universe has always been one of the main topics discussed in the literature. The importance of PBH constraints is that they can provide a clear picture of the number density of PBHs and their contribution to dark matter. In addition to all those observational constraints that have been placed on the abundance of PBHs, the merger rate of these black holes can potentially lead to a constraint on the PBH fraction in dark matter. In particular, the fraction of PBHs is represented by $0 < f_{\text{PBH}} \leq 1$, which indicates their contribution to dark matter.

Nowadays, most of the PBH mass ranges have been

constrained due to the various cosmological processes [21]. There is only a small window, known as the asteroid-mass PBHs [64–69], that is still open. This mass range of PBHs could potentially contain a significant fraction of dark matter. Fortunately, the black hole merger events recorded by the LIGO detectors are a convenient and accessible criterion to evaluate the validity of PBH mergers generated by various halo models. On the other hand, comparing the PBH merger rate obtained from the halo models with the reported mergers by the LIGO detectors leads to a constraint on the fraction of PBHs. Note that, the arising constraints from the merger rate of PBHs in theoretical models are the upper limits that are allowed by the gravitational wave detectors, since the black hole mergers with astrophysical origins are also likely to be recorded by the LIGO detectors.

On the other hand, according to the criterion related to the evaporation time of dark matter halos containing PBHs, one can constrain the smallest halos that have not yet evaporated by the present-time Universe. In fact, the lower limit of the halo mass directly depends on the mass of PBHs located in the host halos (see, e.g., Ref. [25]). The main idea is to find out whether the merger rate and the fraction of PBHs modify with their smaller or larger masses than $30 M_{\odot}$. Under these assumptions, the merger rate for the various masses of PBHs can be calculated. In Table II, we have shown the total merger rate of PBHs for several masses of PBHs while considering the SIDM halo models for $\Delta t = 4$ Gyr after the halo virialization. As it is clear, the merger rate of PBHs is inversely proportional to their masses.

In Fig. 7, we have illustrated the total merger rate of PBHs with respect to their fraction and masses while considering the SIDM halo models for $\Delta t = 4$ Gyr after the halo virialization. In this figure, the shaded band indicates the total merger rate of black holes recorded by

TABLE II: The total merger event rate of PBHs with different masses, i.e., $M_{\text{PBH}} = 10, 20, 50, \text{ and } 100 M_{\odot}$, for the SIDM halo models for $\Delta t = 4$ Gyr after the halo virialization time. The results are related to the present-time Universe.

PBH Mass (M_{\odot})	Total Merger Rate ($\text{Gpc}^{-3}\text{yr}^{-1}$)
10	15.63
20	11.96
50	7.63
100	6.01

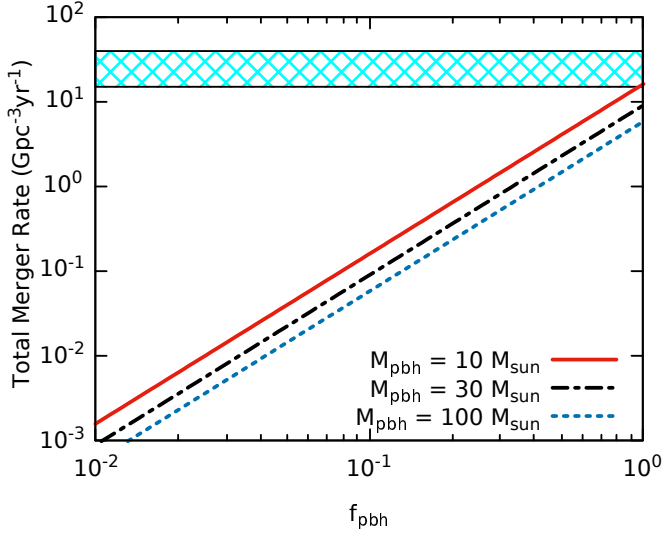


FIG. 7: (color online) The total merger event rate of PBHs for the SIDM halo models after $\Delta t = 4$ Gyr from the halo virialization time with respect to the PBH fraction and mass. The solid (red) line, the dot-dashed (black) line and the dotted (blue) line show this relation considering the PBH mass of $M_{\text{PBH}} = 10, 30, \text{ and } 100 M_{\odot}$, respectively. The shaded (cyan) band is the total merger rate of black holes estimated by the aLIGO detectors during the third observing run, i.e., $15.3 - 38.8 \text{ Gpc}^{-3}\text{yr}^{-1}$.

the aLIGO detectors during the third observing run, i.e., $15.3 - 38.8 \text{ Gpc}^{-3}\text{yr}^{-1}$ [61]. As can be seen, the merger rate of PBHs changes inversely with their masses. Interestingly, despite all theoretical uncertainties, the merger rate of PBHs with a mass of $10 M_{\odot}$ falls within the aLIGO merger range, whereas the corresponding result for the PBH mass ranges of $10 M_{\odot} < M_{\text{PBH}} < 100 M_{\odot}$ will not be located at this window if the CDM halo models are trusted. Given that the spherical-collapse halo mass function is considered for the both models, this result can be mentioned as a relative advantage of the SIDM halo models compared to the CDM ones. In other words, it can be inferred that the SIDM scenario may eliminate the weakness of the spherical-collapse halo models to generate enough PBH mergers to account for the aLIGO mergers.

Thus, $10 M_{\odot} - 10 M_{\odot}$ events can be highlighted as an outstanding result obtained from the SIDM halo models, as such events are consistent with the aLIGO window for $f_{\text{PBH}} \simeq 1$. In other words, within the context of a

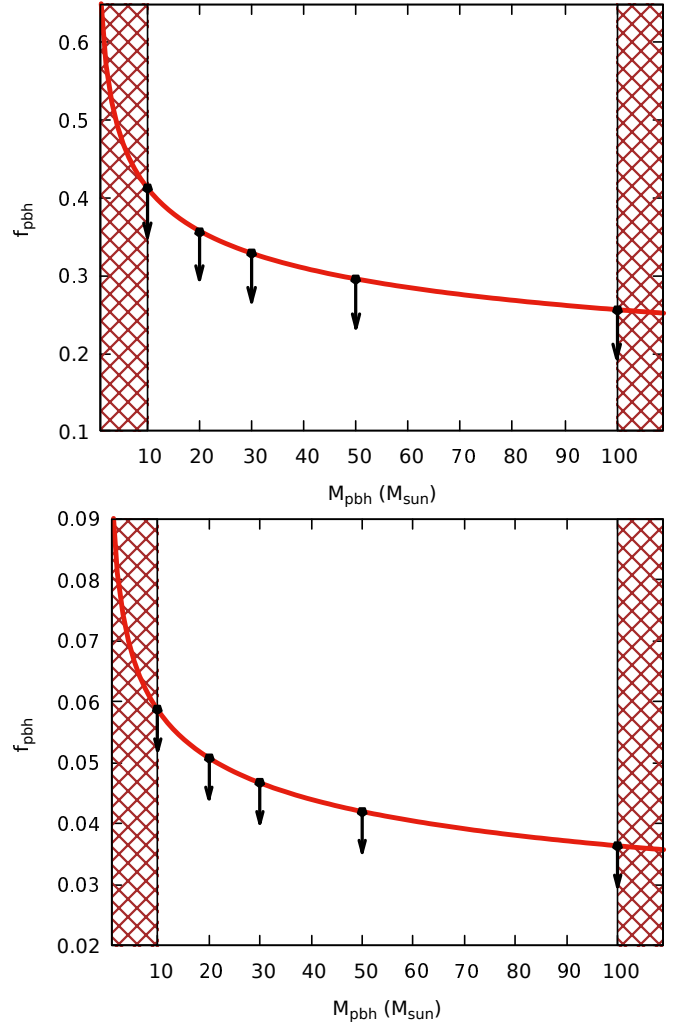


FIG. 8: (color online) The expected upper bounds on the fraction of PBHs, f_{PBH} , as a function of their masses, $10 M_{\odot} < M_{\text{PBH}} < 100 M_{\odot}$ and considering the SIDM halo models for $\Delta t = 4$ Gyr after the halo virialization. The top plot has been quantitated for the situation in which one should expect to detect at least one $30 M_{\odot} - 30 M_{\odot}$ event in the comoving volume 1 Gpc^3 annually, whereas the bottom plot has been calibrated for the same event, but in the comoving volume 50 Gpc^3 .

spherical-collapse halo model, the results of the SIDM scenario suggest that, during the second epoch (e.g., $\Delta t = 4$ Gyr after the halo virialization), sufficient PBH mergers can be generated to reach the aLIGO mergers

if a significant fraction of dark matter could be made of PBHs. Whereas such results would not be the case in the CDM scenario for any value of $f_{\text{PBH}} \leq 1$ and for any value of the PBH mass. It can be inferred from these results that the spherical-collapse halo model is still a suitable model to generate enough PBH mergers to account for aLIGO mergers while considering the SIDM scenario.

As mentioned, the aLIGO detectors can search for the black hole merger events up to a comoving volume around 50 Gpc^3 . Roughly speaking, by considering the SIDM scenario indicated in Fig. 7, the aLIGO detectors are expected to detect about 750 - 800 events annually with $f_{\text{PBH}} \leq 1$. Also, the expected value for the PBH fraction must be $f_{\text{PBH}} > 0.1$ if the number of events would be at least 10 over one year, whereas for the detection of at least one event during the same time, the PBH fraction is predicted to be $f_{\text{PBH}} > 0.01$. It is important to note that the constraints obtained from the merger rate of PBHs within the context of the SIDM halo models can be potentially stronger than the corresponding results inferred from the CDM halo models.

As a final point, let us estimate how the constraints change with different PBH masses. For this purpose, according to the results obtained in Refs. [22, 70], a relation between the fraction of PBHs and their masses can be estimated to be $f_{\text{PBH}} \sim (M_{\text{PBH}}/30 M_{\odot})^{-0.207}$, which is well consistent with the results obtained in this work. In Fig. 8, we have depicted the expected upper bounds on the fraction of PBHs in terms of their masses, while considering the SIDM halo models for $\Delta t = 4 \text{ Gyr}$ after the halo virialization. As can be seen, the fraction of PBHs is inversely proportional to their masses. The top plot represents the situation in which one can expect to record at least one $30 M_{\odot} - 30 M_{\odot}$ event in the comoving volume 1 Gpc^3 annually, while the bottom plot shows the corresponding results for the same event, but in the comoving volume 50 Gpc^3 . Also, to represent the relative differences between the various results, several upper bounds on the fraction of PBHs obtained for some PBH masses have been denoted. Specifically, within the context of the SIDM halo models for $\Delta t = 4 \text{ Gyr}$ after the halo virialization, the fraction of PBHs should be of the order $\mathcal{O}(10^{-1})$ if one expect to detect at least one $30 M_{\odot} - 30 M_{\odot}$ event per year in the comoving volume 1 Gpc^3 , while if the same event occurs in the comoving volume 50 Gpc^3 , the fraction of PBHs is predicted to be of the order $\mathcal{O}(10^{-2})$.

IV. CONCLUSIONS

There are several candidates for dark matter that have been proposed in cosmology and particle physics. As dark matter makes up nearly five times the contribution of baryonic matter, it would not be extraordinary to assume that dark matter itself includes a combination for various candidates. The PBHs and SIDM are two can-

didates of these suggestions. The idea of considering a proportional of dark matter having non-negligible cross section per unit mass of particles and being able to interact with the other dark matter particles can resolve many astrophysical problems, such as the missing satellite and the core-cusp problems. On the other hand, the cutting edge of gravitational-waves detection in the LIGO detectors has started a new era of cosmology in recent years. In particular, studying binary black hole mergers has rapidly been developed as nowadays we have access to direct observational data.

In this work, we have studied the merger rate of PBHs in the SIDM halo models. For this purpose, we have used the result of a previously performed simulation of SIDM with $\sigma/m = 10 \text{ cm}^2\text{g}^{-1}$ to specify a numerical description for the density profile of the SIDM halos as a function of time Δt after the halo virialization. Then, in order to justify the evolution of the density profile in two different epochs (i.e., $\Delta t \leq 1 \text{ Gyr}$ and $\Delta t > 1 \text{ Gyr}$) after the halo virialization, we have proposed two relations for the density profile within the context of the SIDM halo models. In this regard, we have also found a relation for the concentration parameter, time and virialized mass of halo, which can justify the behavior of the evolution of the halo density related to the SIDM halo models.

Furthermore, we have investigated the encounter condition of PBHs that may have been distributed in the medium of dark matter halos randomly. Under these assumptions, we have calculated the merger rate of PBHs per each halo considering the SIDM halo models and have compared the results with the corresponding one obtained for the CDM halo models. Behaviorally, it has been observed that the merger rate of PBHs in the both models is directly proportional to the halo mass. Also, the results indicate that the merger rate of PBHs for the SIDM halo models during the first epoch ($\Delta t \leq 1 \text{ Gyr}$ after the halo virialization) should be lower than the one extracted from the CDM halo models. However, over time and entering the second epoch ($\Delta t > 1 \text{ Gyr}$ after the halo virialization), the inability to generate sufficient PBH mergers in the SIDM halo models is compensated and even exceeds the ones resulted from the CDM halo models. Explicitly, this result is due to the time evolution of the density profile in the SIDM halo models.

In addition, by considering the P-S halo mass function, we have calculated the merger rate of PBHs per unit volume and per unit time for the SIDM halo models and have compared the results with the corresponding findings of the CDM halo models. According to the exponential term in the halo mass function, it has been observed that the cumulative merger rate of PBHs decreases with increasing the halo mass in the both models. The main reason for such behavior is to reduce the dark matter concentration and increase its velocity dispersion in the larger halos. For this reason, the role of the smallest halos is much more prominent than that of the larger halos in a way that the merger rate of PBHs depends significantly on the choice of the lower limit of the halo mass. It has

also been confirmed that the cumulative merger rate of PBHs for the SIDM halo models during the first epoch is lower than the results obtained from the CDM halo models, whereas, in the second epoch, the total merger rate of PBHs is strengthened and exceeds the corresponding result of the CDM halo models.

The possibility of binary PBH formation over the age of the Universe due to their random distribution is a good motivation to examine the evolution of the PBH merger rate as a function of redshift. Accordingly, the results indicate that the total merger rate of PBHs is directly related to the redshift in the both models. In other words, the PBHs have been more likely to form binaries at higher redshifts than the present-time Universe. It needs to be highlighted that the PBH merger rate in the SIDM halo models during the first epoch is always lower than the results obtained in the CDM halo models, while over time, compared to the halo virialization and entering the second epoch, the total merger rate is compensated and exceeds the value obtained in the CDM halo models. Also, when the total merger rate is more considerable (i.e., after the core collapse in the SIDM halo models), the slope of difference as a function of redshift is larger than the one obtained for the CDM halo models.

Finally, to determine the constraint of PBHs, we have studied the merger rate of PBHs concerning their masses and fraction and have compared those with the mergers estimated by the aLIGO detectors during the third observing run, i.e., $15.3 - 38.8 \text{ Gpc}^{-3}\text{yr}^{-1}$. The results for the CDM halo models and for the SIDM halo models during the first epoch are not promising in a way that those do not fall into the aLIGO window for any value of $f_{\text{PBH}} \leq 1$. Whereas the situation is slightly different for the SIDM halo models during the second epoch in a way that the merger rates move closer to the aLIGO window. Eventually, it has been observed that within the context of the SIDM halo models during the second epoch, the merger rate of $10 M_{\odot} - 10 M_{\odot}$ events will enter in the aLIGO window if $f_{\text{PBH}} \simeq 1$.

Given the sensitivity of the aLIGO detectors to probe events up to $z \sim 0.75$ (corresponding to 50 Gpc^3), and in

terms of the obtained results for the SIDM halo models during the second epoch, it is expected that the aLIGO detectors could record about 750 - 800 events annually with $f_{\text{PBH}} \simeq 1$. Also, the number of events should be at least 10 over one year if $f_{\text{PBH}} > 0.1$, and for the detection of at least one event during the same time, the PBH fraction is predicted to be $f_{\text{PBH}} > 0.01$. We have also estimated a relation for the fraction of PBHs and their masses, which is consistent with the results obtained in this work. According to the merger rates obtained for different PBH masses, it has been observed that the fraction of PBHs varies inversely with their masses.

In addition to the PBH constraint obtained in this work, other strong observational constraints have been imposed to the stellar-mass PBHs that come from the gravitational lensing of type Ia supernovae [71], the Planck data on the cosmic microwave background anisotropies [72, 73], dynamical processes from star clusters in nearby dwarf galaxies [74, 75], and the accretion limits from the observed number of x-ray binaries [76].

It should also be noted that the constraint of PBHs is subject to many uncertainties, including different dark matter scenarios (e.g., the CDM or the SIDM), different conditions that may have imposed on the structures during those collapse and formation, some processes that may lead to the growth (e.g., accretion and merger history) or evaporation (e.g., substantial spin) of PBHs, uncertainties arising from the black hole formation scenarios and their contribution to the LIGO mergers, and mass distribution of PBHs. Although the presence of such factors may lead to computational errors, with the development of the instrument and a better understanding of unknown processes, one could attain stronger constraints on PBHs in the future.

ACKNOWLEDGMENTS

S.F. and M. F. thank the Research Council of Shahid Beheshti University.

-
- [1] B.P. Abbott *et al.* [LIGO Scientific and Virgo Collaborations], “Observation of gravitational waves from a binary black hole merger”, *Phys. Rev. Lett.* **116**, 061102 (2016).
 - [2] B.P. Abbott *et al.* [LIGO Scientific and Virgo Collaborations], “GW151226: Observation of gravitational waves from a 22-solar-mass binary black hole coalescence”, *Phys. Rev. Lett.* **116**, 241103 (2016).
 - [3] B.P. Abbott *et al.* [LIGO Scientific and Virgo Collaborations], “GW170817: Observation of gravitational waves from a binary neutron star inspiral”, *Phys. Rev. Lett.* **119**, 161101 (2017).
 - [4] B.P. Abbott *et al.* [LIGO Scientific and Virgo Collaborations], “Tests of general relativity with GW150914”, *Phys. Rev. Lett.* **116**, 221101 (2016); Erratum: *Phys. Rev. Lett.* **121**, 129902 (2018).
 - [5] R. Abbott *et al.* [LIGO Scientific and Virgo Collaborations], “GW190814: Gravitational waves from the coalescence of a 23 solar mass black hole with a 2.6 solar mass compact object”, *Astrophys. J. Lett.* **896**, L44 (2020).
 - [6] R. Abbott *et al.* [LIGO Scientific and Virgo Collaborations], “GW190521: A binary black hole merger with a total mass of $150 M_{\odot}$ ”, *Phys. Rev. Lett.* **125**, 101102 (2020).
 - [7] M. Fishbach *et al.*, “When are LIGO/Virgo’s big black hole mergers?”, *Astrophys. J.* **912**, 98 (2021).
 - [8] C.L. Rodriguez *et al.*, “The observed rate of binary black hole mergers can be entirely explained by globular clusters”, *Res. Notes AAS* **5**, 19 (2021).
 - [9] Y.B. Zel’dovich and I.D. Novikov, “The hypothesis of cores retarded during expansion and the hot cosmolog-

- ical model”, *Soviet Astron. AJ (Engl. Transl.)* **10**, 602 (1967).
- [10] B.J. Carr, “The primordial black hole mass spectrum”, *Astrophys. J.* **201**, 1 (1975).
- [11] J.C. Niemeyer and K. Jedamzik, “Dynamics of primordial black hole formation”, *Phys. Rev. D* **59**, 124013 (1999).
- [12] M. Shibata and M. Sasaki, “Black hole formation in the Friedmann universe: Formulation and computation in numerical relativity”, *Phys. Rev. D* **60**, 084002 (1999).
- [13] A.G. Polnarev and I. Musco, “Curvature profiles as initial conditions for primordial black hole formation”, *Class. Quant. Grav.* **24**, 1405 (2007).
- [14] I. Musco and J.C. Miller, “Primordial black hole formation in the early universe: Critical behaviour and self-similarity”, *Class. Quant. Grav.* **30**, 145009 (2013).
- [15] S. Young, C.T. Byrnes and M. Sasaki, “Calculating the mass fraction of primordial black holes”, *J. Cosmol. Astropart. Phys.* **1407**, 045 (2014).
- [16] J. Bloomfield, D. Bulhosa and S. Face, “Formalism for primordial black hole formation in spherical symmetry”, arXiv:1504.02071.
- [17] A. Allahyari, J.T. Firouzjaee and A.A. Abolhasani, “Primordial black holes in linear and non-linear regimes”, *J. Cosmol. Astropart. Phys.* **1706**, 041 (2017).
- [18] B. Carr and F. Kühnel, “Primordial black holes as dark matter: Recent developments”, *Annu. Rev. Nucl. Part. Sci.* **70**, 355 (2020).
- [19] B. Carr, M. Raidal, T. Tenkanen, V. Vaskonen and H. Veermäe, “Primordial black hole constraints for extended mass functions”, *Phys. Rev. D* **96**, 023514 (2017).
- [20] B.V. Lehmann, S. Profumo and J. Yant, “The maximal-density mass function for primordial black hole dark matter”, *J. Cosmol. Astropart. Phys.* **1804**, 007 (2018).
- [21] B. Carr, K. Kohri, Y. Sendouda and J. Yokoyama, “Constraints on primordial black holes”, arXiv:2002.12778.
- [22] S. Bird, *et al.*, “Did Ligo detect dark matter?”, *Phys. Rev. Lett.* **116**, 201301 (2016).
- [23] S. Clesse and J. García-Bellido, “The clustering of massive primordial black holes as dark matter: Measuring their mass distribution with Advanced LIGO”, *Phys. Dark Univ.* **15**, 142-147 (2017).
- [24] M. Sasaki, T. Suyama, T. Tanaka and S. Yokoyama, “Primordial black hole scenario for the gravitational-wave event GW150914”, *Phys. Rev. Lett.* **117**, 061101 (2016); Erratum: *Phys. Rev. Lett.* **121**, 059901 (2018).
- [25] S. Fakhry, J.T. Firouzjaee and M. Farhoudi, “Primordial black hole merger rate in ellipsoidal-collapse dark matter halo models”, *Phys. Rev. D* **103**, 123014 (2021).
- [26] D.N. Spergel and P.J. Steinhardt, “Observational evidence for self-interacting cold dark matter”, *Phys. Rev. Lett.* **84**, 3760 (2000).
- [27] B. Moore *et al.* “Dark matter substructure within galactic halos”, *Astrophys. J. Lett.* **524**, L19 (1999).
- [28] J. Bullock, “Notes on the missing satellites problem”, (Cambridge University Press, Cambridge, 2013).
- [29] N. Bernal and Ó. Zapata, “Self-interacting dark matter from primordial black holes”, *J. Cosmol. Astropart. Phys.* **03**, 007 (2021).
- [30] A. Loeb and N. Weiner, “Cores in dwarf galaxies from dark matter with a Yukawa potential”, *Phys. Rev. Lett.* **106**, 171302 (2011).
- [31] J.F. Navarro, C.S. Frenk and S.D.M. White, “A universal density profile from hierarchical clustering”, *Astrophys. J.* **490**, 493 (1997).
- [32] G.L. Bryan and M.L. Norman, “Statistical properties of x-ray clusters: Analytic and numerical comparisons”, *Astrophys. J.* **495**, 80 (1998).
- [33] M.S. Fischer *et al.*, “N-body simulations of dark matter with frequent self-interactions”, *Mon. Not. Roy. Astron. Soc.* **505**, 851 (2021).
- [34] T. Brinckmann, J. Zavala, D. Rapetti, S.H. Hansen and M. Vogelsberger, “The structure and assembly history of cluster-sized haloes in self-interacting dark matter”, *Mon. Not. Roy. Astron. Soc.* **474**, 746 (2018).
- [35] F. Prada *et al.*, “Halo concentrations in the standard Λ cold dark matter cosmology”, *Mon. Not. Roy. Astron. Soc.* **423**, 3018 (2012).
- [36] A.A. Dutton and A.V. Macciò, “Cold dark matter haloes in the Planck era: Evolution of structural parameters for Einasto and NFW profiles”, *Mon. Not. Roy. Astron. Soc.* **441**, 3359 (2014).
- [37] C. Okoli and N. Afshordi, “Concentration, ellipsoidal collapse, and the densest dark matter haloes”, *Mon. Not. Roy. Astron. Soc.* **456**, 3068 (2016).
- [38] A.D. Ludlow *et al.*, “The mass-concentration-redshift relation of cold and warm dark matter haloes”, *Mon. Not. Roy. Astron. Soc.* **460**, 1214 (2016).
- [39] A.V. Macciò, A.A. Dutton and F.C.v.d. Bosch, “Concentration, spin and shape of dark matter haloes as a function of the cosmological model: WMAP1, WMAP3 and WMAP5 results”, *Mon. Not. Roy. Astron. Soc.* **391**, 1940 (2008).
- [40] K. Bondarenko, A. Boyarsky, T. Bringmann and A. Sokolenko, “Constraining self-interacting dark matter with scaling laws of observed halo surface densities”, *J. Cosmol. Astropart. Phys.* **04**, 049 (2018).
- [41] M. Naseri and J.T. Firouzjaee, “Super interacting dark sector: An improvement on self-interacting dark matter via scaling relations of galaxy clusters”, arXiv:2011.07718.
- [42] L. Sagunski, S. Gad-Nasr, B. Colquhoun, A. Robertson and S. Tulin, “Velocity-dependent self-interacting dark matter from groups and clusters of galaxies”, *J. Cosmol. Astropart. Phys.* **01**, 024 (2021).
- [43] O. Lahav, P.B. Lilje, J.R. Primack and M.J. Rees, “Dynamical effects of the cosmological constant”, *Mon. Not. Roy. Astron. Soc.* **251**, 128 (1991).
- [44] Z. Lukic, K. Heitmann, S. Habib, S. Bashinsky and P. M. Ricker, “The halo mass function: High redshift evolution and universality”, *Astrophys. J.* **671**, 1160 (2007).
- [45] D. Reed, R. Bower, C. Frenk, A. Jenkins and T. Theuns, “The halo mass function from the dark ages through the present day”, *Mon. Not. Roy. Astron. Soc.* **374**, 2 (2007).
- [46] S. Murray, C. Power and A. Robotham, “How well do we know the halo mass function?”, *Mon. Not. Roy. Astron. Soc.* **434**, L61 (2013).
- [47] A. Jenkins, C.S. Frenk, S.D.M. White, J.M. Colberg, S. Cole, A.E. Evrard, H.M.P. Couchman and N. Yoshida, “The mass function of dark matter halos”, *Mon. Not. Roy. Astron. Soc.* **321**, 372 (2001).
- [48] W.H. Press and P. Schechter, “Formation of galaxies and clusters of galaxies by self-similar gravitational condensation”, *Astrophys. J.* **187**, 425 (1974).
- [49] R.K. Sheth, H.J. Mo and G. Tormen, “Ellipsoidal collapse and an improved model for the number and spatial distribution of dark matter haloes”, *Mon. Not. Roy. As-*

- tron. Soc.* **323**, 1 (2001).
- [50] D. Reed, *et al.*, “Evolution of the mass function of dark matter haloes”, *Mon. Not. Roy. Astron. Soc.* **346**, 565 (2003).
- [51] M.S. Warren, K. Abazajian, D.E. Holz and L. Teodoro, “Precision determination of the mass function of dark matter halos”, *Astrophys. J.* **646**, 881 (2006).
- [52] A.H.G. Peter, M. Rocha, J.S. Bullock and M. Kaplinghat, “Cosmological simulations with self-interacting dark matter ii: Halo shapes vs. observations”, *Mon. Not. Roy. Astron. Soc.* **430**, 105 (2013).
- [53] P.C. Peters, “Gravitational radiation and the motion of two point masses”, *Phys. Rev.* **136**, B1224 (1964).
- [54] M. Sasaki, T. Suyama, T. Tanaka and S. Yokoyama, “Primordial black holes—perspectives in gravitational wave astronomy”, *Class. Quant. Grav.* **35**, 063001 (2018).
- [55] G.D. Quinlan and S.L. Shapiro, “Dynamical evolution of dense clusters of compact stars”, *Astrophys. J.* **343**, 725 (1989).
- [56] H. Mouri and Y. Taniguchi, “Runaway merging of black holes: Analytical constraint on the timescale”, *Astrophys. J. Lett.* **566**, L17 (2002).
- [57] H. Nishikawa, E.D. Kovetz, M. Kamionkowski and J. Silk, “Primordial-black-hole mergers in dark-matter spikes”, *Phys. Rev. D* **99**, 043533 (2019).
- [58] A. Robertson *et al.* “Observable tests of self-interacting dark matter in galaxy clusters: Cosmological simulations with SIDM and baryons”, *Mon. Not. Roy. Astron. Soc.* **488**, 3646 (2019).
- [59] M. Kamionkowski and S.M. Koushiappas, “Galactic substructure and direct detection of dark matter”, *Phys. Rev. D* **77**, 103509 (2008).
- [60] B.P. Abbott *et al.* [LIGO Scientific and Virgo Collaborations], “Binary black hole population properties inferred from the first and second observing runs of Advanced LIGO and Advanced Virgo”, *Astrophys. J. Lett.* **882**, L24 (2019).
- [61] R. Abbott *et al.* [LIGO Scientific and Virgo Collaborations], “GWTC-2: Compact binary coalescences observed by LIGO and Virgo during the first half of the third observing run”, arXiv:2010.14527.
- [62] V. Mandic, S. Bird and I. Cholis, “Stochastic gravitational-wave background due to primordial binary black hole mergers”, *Phys. Rev. Lett.* **117**, 201102 (2016).
- [63] A.D. Gow, C.T. Byrnes, A. Hall and J.A. Peacock, “Primordial black hole merger rates: Distributions for multiple LIGO observables”, *J. Cosmol. Astropart. Phys.* **01**, 031 (2020).
- [64] A. Katz, J. Kopp, S. Sibiryakov and W. Xue, “Femtolensing by dark matter revisited”, *J. Cosmol. Astropart. Phys.* **12**, 005 (2018).
- [65] P. Montero-Camacho, X. Fang, G. Vasquez, M. Silva and C.M. Hirata, “Revisiting constraints on asteroid-mass primordial black holes as dark matter candidates”, *J. Cosmol. Astropart. Phys.* **08**, 031 (2019).
- [66] N. Smyth *et al.*, “Updated constraints on asteroid-mass primordial black holes as dark matter”, *Phys. Rev. D* **101**, 063005 (2020).
- [67] A. Coogan, L. Morrison and S. Profumo, “Direct detection of Hawking radiation from asteroid-mass primordial black holes”, *Phys. Rev. Lett.* **126**, 171101 (2021).
- [68] A. Ray, R. Laha, J.B. Muñoz and R. Caputo, “Closing the gap: Near future MeV telescopes can discover asteroid-mass primordial black hole dark matter”, arXiv:2102.06714.
- [69] Z.S.C. Picker, “Navigating the asteroid field: New evaporation constraints for primordial black holes as dark matter”, arXiv:2103.02815.
- [70] Y. Ali-Haïmoud, E.D. Kovetz and M. Kamionkowski, “Merger rate of primordial black-hole binaries”, *Phys. Rev. D* **96**, 123523 (2017).
- [71] M. Zumalacarregui and U. Seljak, “Limits on stellar-mass compact objects as dark matter from gravitational lensing of type Ia supernovae”, *Phys. Rev. Lett.* **121**, 141101 (2018).
- [72] Y. Ali-Haïmoud and M. Kamionkowski, “Cosmic microwave background limits on accreting primordial black holes”, *Phys. Rev. D* **95**, 043534 (2017).
- [73] P.D. Serpico, V. Poulin, D. Inman and K. Kohri, “Cosmic microwave background bounds on primordial black holes including dark matter halo accretion”, *Phys. Rev. Res.* **2**, 023204 (2020).
- [74] T.D. Brandt, “Constraints on MACHO dark matter from compact stellar systems in ultra-faint dwarf galaxies”, *Astrophys. J. Lett.* **824**, L31 (2016).
- [75] S.M. Koushiappas and A. Loeb, “Dynamics of dwarf galaxies disfavor stellar-mass black holes as dark matter”, *Phys. Rev. Lett.* **119**, 041102 (2017).
- [76] Y. Inoue and A. Kusenko, “New x-ray bound on density of primordial black holes”, *J. Cosmol. Astropart. Phys.* **10**, 034 (2017).